DC microgrid power coordination based on fuzzy logic control

AL BADWAWI, Rashid, ISSA, Walid <http://orcid.org/0000-0001-9450-5197>, MALLICK, Tapas and ABUSARA, Mohammad

DC microgrid power coordination based on fuzzy logic control

Conference Paper · September 2016

DOI: 10.1109/EPE.2016.7695530

4 authors, including:

Rashid Al Badwawi
Oman Electricity Transmission Company
16 PUBLICATIONS **20** CITATIONS
SEE PROFILE

Walid Issa
Sheffield Hallam University
14 PUBLICATIONS **26** CITATIONS
SEE PROFILE

Tapas K Mallick
University of Exeter
222 PUBLICATIONS **1,686** CITATIONS
SEE PROFILE

DC Microgrid Power Coordination Based on Fuzzy Logic Control

Rashid Al Badwawi*, Walid Issa, Tapas Mallick, and Mohammad Abusara
Environment and Sustainability Institute, University of Exeter
Penryn Campus, TR10 9FE
Penryn, UK
Tel.: +44 / (01326) – 259.478.
*E-Mail: rsma202@exeter.ac.uk
URL: http://www.exeter.ac.uk/esi/

Acknowledgements

The work is financially supported by the Government of Oman, which provides a PhD grant for Rashid Al Badwawi. Also, the work is supported by EPSRC-DST funded project: Reliable and Efficient System for Community Energy Solutions (RESCUES- EP/K03619X/1).

Keywords

«Microgrid», «Power management», «Fuzzy control», «Energy storage», «Renewable energy systems».

Abstract

The power coordination in DC microgrids has a vital role in enhancing the performance and management of multi generation units. Renewable Energy Sources (RES) are limited to their available power with intermittent nature. Battery-based energy storage sources have limitations in the charging and discharging capabilities to avoid depleting the battery and preserve the State of Charge (SOC) within its satisfactory limits. The battery balances the power difference between RES and loads. However, in severe cases where the SOC is very low, load shedding is crucial. In this paper, a Fuzzy Logic Controller (FLC) has been proposed to coordinate the power flow of PV unit and battery to satisfy the load by full use of the available PV power. It controls the PV's output power and keeps the SOC and charging / discharging power of the battery within their required margins regardless of the variations in load. Furthermore, load shedding of low priority load has been implemented when the battery couldn't balance the microgrid power flow. Simplicity in managing multi input-multi output system by FLC is the main merit. Matlab/Simulink results are presented to validate the performance of the proposed controller.

Introduction

Renewable energy sources become preferable option for powering areas that are not connected to main grid. Energy Storage System (ESS) such as battery is essential to balance the power flow between the microgrid elements (generations and loads). Furthermore, it provides more reliability to the microgrid especially for working in different modes of operation; grid-connected or island modes. Although AC microgrid [1] is more dominant in terms of research and existence compared to DC microgrid; DC microgrid starts getting more attention and consideration due to its higher efficiency. In addition, some of the issues that are faced in AC microgrids like reactive power flow, power quality, and frequency control are not issues in DC microgrids. This in turn makes the corresponding primary control notably less complex than its equivalent AC version [2]. Energy management and control design is one of the challenges for microgrids with RES systems along with Battery Energy Storage System (BESS) [3], [4]. However, in the last couple of years, the interest on designing rule-based microgrid' supervisory controller increased to provide a proper power management of different power generation units, including renewable energy sources. In line with this direction, researchers worldwide adopted Fuzzy Logic Controller (FLC) for energy management in both standalone and grid-connected hybrid

renewable energy systems. As per the literature, FLC has been used in both DC and AC microgrids, whether in standalone or grid-connected mode of operations, for several purposes such as maximum power point tracking (MPPT) of solar PV and/or wind power systems [5]–[7], controlling batteries' output charge current [8], etc. FLC was used to manage the state of charge (SOC) of a Li-ion battery connected to a DC microgrid with solar photovoltaic (PV), wind and fuel cell system [9]. The FLC provides the output current for charging or discharging the battery. By adjusting the droop coefficient of primary controllers in a DC microgrid, a decentralized fuzzy logic gain-scheduling controller was proposed in [10] in order to balance the stored energy between different batteries' systems. To improve the performance of a hybrid microgrid generation system with smaller energy capacity of BESS, the SOC of the BESS was controlled by FLC in [11]. FLC has been also used in [12] to provide powers' split between solar PV and BESS based on operator's experience through a pre-defined rules in order to supply DC load. The PV power, SOC of the battery and power required by the load are the inputs to the FLC. The output of the FLC decides the operation of the different switches to have one of the possible connections; PVP-battery, battery-load and PVP-load.

In this paper, PV system has been used along with battery system to form a DC microgrid. Unlike most of designed FLCs in the literature, the proposed FLC in this paper is divided into two subsystems to simplify the design. One subsystem is responsible for preventing the battery SOC and charging power from exceeding their maximum design limits or overcharging. The output of the FLC decides whether to use the maximum power from PV or curtail it according to the SOC, the charging / discharging power and the load. On the other hand, the second subsystem is responsible for preventing the battery SOC from exceeding its minimum design limit and the discharging power from its maximum value. At the same time, the output of the FLC decides the load shedding switches operation to decide to supply the whole loads or go for load shedding whenever required. The FLC is designed for efficient use of the PV and battery powers to keep the SOC and charging/ discharging power of the battery within their required margins regardless of variation in load and intermittent power. Matlab/Simulink results validated the performance of the proposed FLC.

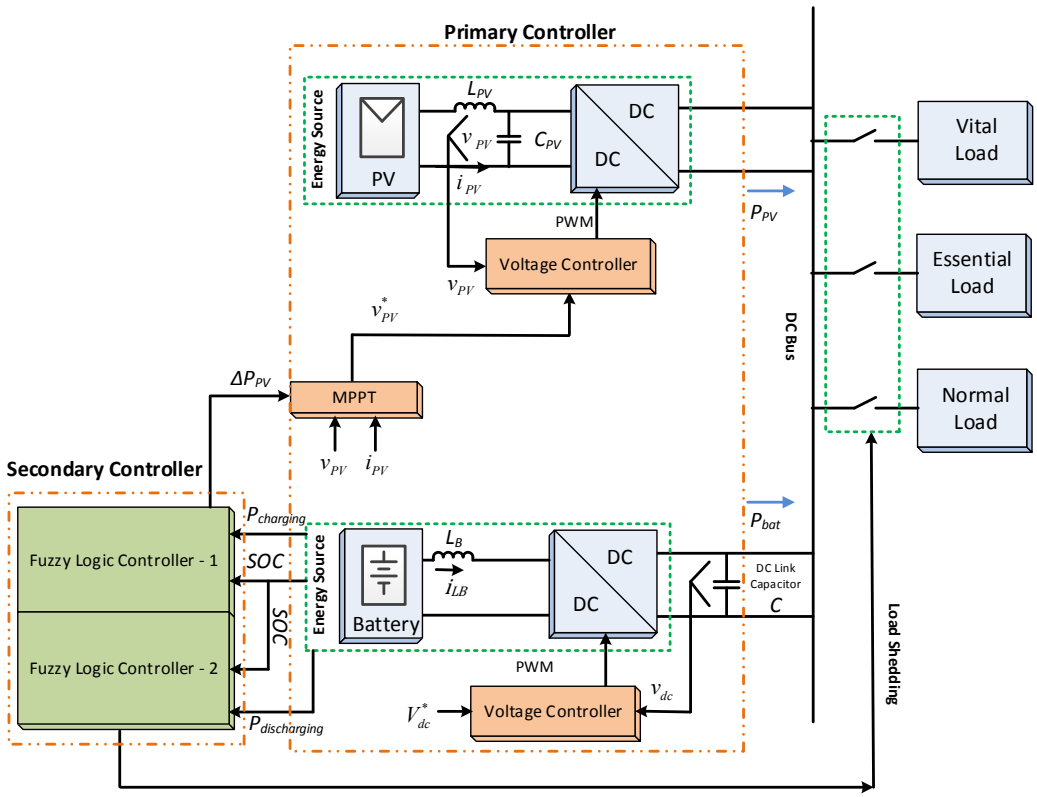

Fig. 1: Microgrid structure

Microgrid structure

The main microgrid structure under consideration in this paper is shown in Fig.1 in islanded mode. It consists of a renewable energy source represented by PV unit and an energy storage system represented by a battery bank. The operation of both generation units is as follows.

1. PV unit exports power to the common DC bus according to MPPT command via a unidirectional DC/DC converter. The latter controls the PV's output voltage to achieve MPPT.
2. BESS unit which has a bidirectional DC/DC converter to regulate the DC bus voltage. The BESS is working as a master voltage source to maintain the DC bus stability of the islanded microgrid. A PI controller is embedded in battery system to control the DC bus voltage at 380V.

The control system is divided into two levels separated by control bandwidth. The primary level contains the voltage and current controllers for the DC/DC converters. The latter is designed to have fast disturbance rejection with high bandwidth control loop (i.e. > 500 rad/s) to track the commanded references values. The secondary level is represented by the FLC which is designed to have lower bandwidth. This criterion is a rule of thumb for nested control loops to preserve system stability. The FLC maintains the power flow in the microgrid according to pre-defined rules. The output of it manipulates the references values (voltage or current) of the primary control level.

Primary control loops design

The primary level control loop design of the BESS bidirectional boost converter and PV uni-directional DC/DC converter are as described below. The key parameters of the BESS and PV systems are as shown in Table I.

BESS DC/DC converter

The linearized averaged state-space model for bidirectional boost BESS DC/DC converter are as follows [13], [14].

$$\begin{bmatrix} \dot{\imath_{LB}} \\ \dot{v_{dc}} \end{bmatrix} = \begin{bmatrix} 0 & \frac{-(1-D)}{L_B} \\ \frac{1-D}{C} & \frac{-1}{RC} \end{bmatrix} \begin{bmatrix} i_{LB} \\ v_{dc} \end{bmatrix} + \begin{bmatrix} \frac{V_{dc}}{L_B} \\ \frac{-I_{LB}}{C} \end{bmatrix} d \tag{1}$$

$$\mathrm{y} = \begin{bmatrix} 1 & 0 \\ 0 & 1 \end{bmatrix} \begin{bmatrix} i_{LB} \\ v_{dc} \end{bmatrix} \tag{2}$$

where L_B, V_{dc}, C and R are the converter inductor, nominal DC-link voltage, DC-link capacitor and equivalent load resistor. I_{LB}, D are the inductor current and averaged duty cycle considered in steady state of the operating point. d is the averaged control input. From (1) and (2), the transfer functions G_{iLB-d} and $G_{vdc-iLB}$ are calculated [14].

$$G_{iLB-d} = \frac{i_{LB}(s)}{d(s)} = \frac{RCV_{dc}s + [(1-D)RI_{LB} + V_{dc}]}{RCL_Bs^2 + L_Bs + R\,(1-D)^2} \tag{3}$$

$$G_{vdc-iLB} = \frac{v_{dc}\,(s)}{i_{LB}(s)} = \frac{-I_{LB}RL_Bs + V_{dc}R(1-D)}{V_{dc}RCs + [V_{dc} + (1-D)I_{LB}R]} \tag{4}$$

The PI controllers of the current loop and voltage loop are as follows:

$$G_{PI-B1(s)} = \frac{0.005s + 1}{s} \tag{5}$$

$$G_{PI-B2(s)} = \frac{s + 50}{s} \tag{6}$$

Based on above, the open-loop and closed-loop bode diagram for the bidirectional boost DC/DC converter is as shown in Fig. 2 where the controller has a gain margin of 46.6 dB and a phase margin of 69.4 deg. The PI controller is also designed to provide a bandwidth of 1580 rad/s. The control system structure for the battery bidirectional boost converter is as shown in Fig. 3.

PV DC/DC converter

The linearized averaged state-space model for unidirectional boost PV DC/DC converter are as follows [13]–[15]:

$$\begin{bmatrix} \dot{i_{Lpv}} \\ \dot{v_{pv}} \end{bmatrix} = \begin{bmatrix} 0 & \frac{1}{L_{PV}} \\ \frac{-1}{C_{pv}} & \frac{1}{r_{pv}C_{pv}} \end{bmatrix} \begin{bmatrix} i_{Lpv} \\ v_{pv} \end{bmatrix} + \begin{bmatrix} V_{dc} \\ 0 \end{bmatrix} d \tag{7}$$

$$\mathrm{y} = \begin{bmatrix} 1 & 0 \\ 0 & 1 \end{bmatrix} \begin{bmatrix} i_{Lpv} \\ v_{pv} \end{bmatrix} \tag{8}$$

where L_{pv}, V_{dc} , C_{pv} and r_{pv} are the converter inductor, nominal DC-link voltage, PV input capacitor and dynamic resistor of the PV at the considered operating point. d is the averaged control input. From (7) and (8), the transfer functions G_{iLpv-d} and $G_{vpv-iLpv}$ are defined [14].

$$G_{iLpv-d} = \frac{i_{Lpv}(s)}{d(s)} = \frac{(C_{pv}r_{pv}s-1)V_{dc}}{L_{pv}C_{pv}r_{pv}s^2 - L_{pv}s+r_{pv}} \tag{9}$$

$$G_{vpv-iLpv} = \frac{v_{pv}\,(s)}{i_{Lpv}(s)} = \frac{-r_{pv}}{C_{pv}r_{pv}s-1} \tag{10}$$

The PI controllers of the current loop and voltage loop are designed as follows:

$$G_{PI-pv1(s)} = \frac{10s + 250}{s} \tag{11}$$

$$G_{PI-pv2(s)} = \frac{0.05s + 1}{s} \tag{12}$$

Based on above, the open-loop and closed-loop bode diagram for the unidirectional boost PV DC/DC converter is as shown in Fig. 4 where the controller has a very high gain margin and a phase margin of 66.6 deg. The bandwidth of the control loop is 745 rad/s. The control system structure for the PV unidirectional boost converter is as shown in Fig. 5.

Table I: Key system parameters

Parameter	Symbol	Value
Equivalent load resistor for BESS DC/DC converter	R	440 Ω
DC output capacitor	C	1100 µF
Nominal DC-link voltage	V_{dc}	380 V
Duty cycle	D	0.25
Inductor current	I_{LB}	0.7 A
BESS and PV converter inductor	L_B, L_{pv}	0.8 mH
PV Dynamic resistor	r_{pv}	-6Ω
PV Input capacitor	C_{pv}	1100 µF

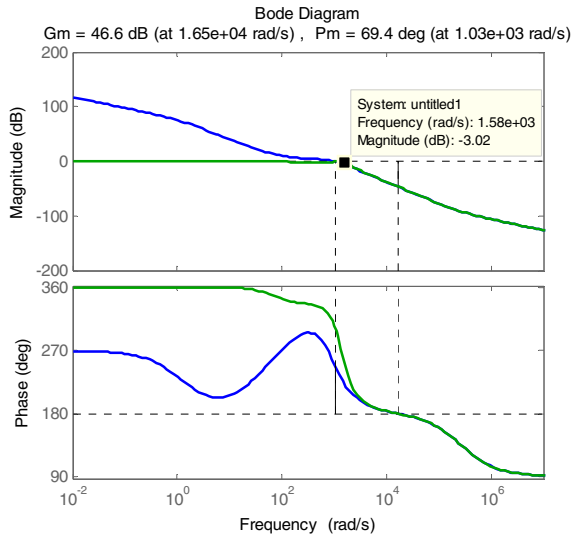

Fig. 2: Open-loop and closed-loop bode diagram for the bidirectional boost BESS DC/DC converter

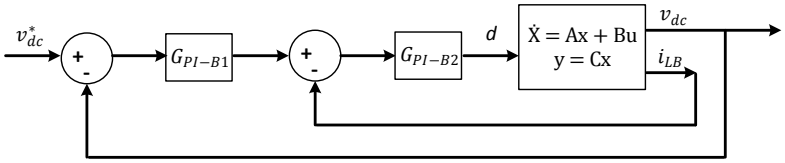

Fig. 3: Control system structure for the battery bidirectional boost BESS DC/DC converter

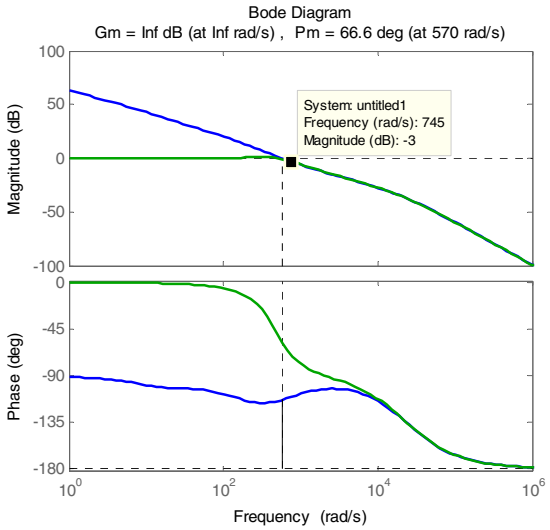

Fig. 4: Open-loop and closed-loop bode diagram for the unidirectional boost PV DC/DC converter

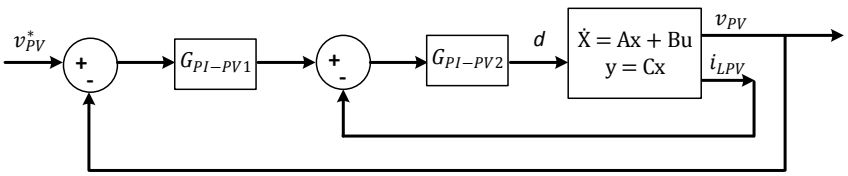

Fig. 5: Control system structure for the unidirectional boost PV DC/DC converter

PV Power shifter

If the power generation from PV is higher than the load, the battery normally absorbs the excess power. However, if the SOC of the BESS is very high, the PV power should be curtailed to prevent overcharging the battery. For the latter objective, a PV power shifter is implemented. Normally, the MPPT controller regulates the voltage across the PV to supply the maximum power. When a curtailment is needed, the power shifter shifts the PV voltage to deviate it from the maximum power point to a lower point as illustrated in Fig. 6(a). The more rise in the PV output voltage; the more curtailment in PV power and vice versa.

Proposed fuzzy logic controller

The proposed FLC is designed to work as a supervisory controller and divided into two subsystems to simplify the design in order to achieve the required objectives. One general objective of the FLC is to control the generated power distribution efficiently between the PV and battery to meet the required load power. The main objective is to protect the battery from overcharging or over discharging with full use of the PV power. The basic FLC is as shown in Fig. 7 and it consists of two subsystems;

1. The top subsystem is designed to limit the battery from overcharging (i.e. keeping the SOC below its maximum limit SOC^{*}_{max}) and also to prevent the maximum charging power from exceeding its limit by curtailing the PV power if needed. The inputs are ΔSOC (difference between current SOC and its maximum value SOC^{*}_{max}) and ΔP_{charge} (difference between charging power and its maximum charging power value $P^{*}_{charge\_max}$). The output is an increase or decrease in the PV power ΔP_{PV} which will be translated by the power shifter as illustrated in Fig. 6(b).
2. The bottom FLC subsystem is designed to limit the battery from over discharging (i.e. keeping the SOC above its minimum limit SOC^{*}_{min}) by shedding some loads whenever required. The inputs are ΔSOC (difference between current SOC and its minimum limit SOC^{*}_{min}) and $\Delta P_{discharge}$ (difference between discharging power and its maximum discharging power value $P^{*}_{discharge\_max}$). The output is a change in load power ΔP_{Load} realized by logic signals that control the state of the loads switches in Fig 1. It is worth mentioning here that the load has been classified to three groups according to its priory: vital (170W), essential (400W) and normal (570W) loads. The normal load shedding will be done first when required. Then if necessary, the essential load shedding will be done next and the last resort in terms of load shedding will be for vital load. The SOC and power limits are shown in Table II.

The rules for the FLC are shown in Table III (top subsystem) and Table IV (bottom subsystem). The terms L, M and H denote low, medium and high membership functions, respectively. The membership functions of top and bottom FLC subsystems are shown in Fig. 8 and Fig. 9 respectively. To satisfy the nested control loop operation, a low pass filer (LPF) is used on the FLC outputs; which provides a slower bandwidth than the primary controllers. Its cut-off frequency is equal to 150 rad/s which is chosen to be 5 times less than the lowest primary control bandwidth.

Simulation results

A DC microgrid as shown in Fig. 1 has been built in Matlab/Simulink with the proposed controllers. For the sake of validating the performance of the proposed FLC in the secondary control level. The bandwidth separation securely supports the assumption of considering ideal current and voltage sources instead of the DC/DC converters. Therefore, in the simulation, ideal current and voltage sources are implemented in the primary level and the reference values obtained from FLC in the secondary level. The FLC is designed in Matlab/Simulink using Fuzzy Logic tool box.

Several cases of battery SOC, PV power and load have been carried out to validate the performance of the proposed FLC. The load and PV power profiles have been defined to cover comprehensive scenarios. Fig. 10(a) shows the power output of the battery and PV systems in addition to the loads' power and SOC curve for initial SOC value of 95%. During each load value, the PV power changes from zero to medium to high generation. The aim is to keep the SOC and charging power within the

maximum limits; otherwise PV generation should be curtailed. At t = 0s, the PV generation was zero and the whole power was supplied by the battery. When the PV power dropped to around 380W at t = 1s, the battery provided the remaining power since the load was higher than PV power until the generated power from the PV increased to 1000W at t = 2s. After that, the PV generation dropped to zero at t = 3s. Hence, the battery supplied the whole power by discharging. The above profile of the PV was repeated again for the period from t = 3s to 6s, but with a lower load. At t = 4s, the PV produced 380W and the battery provided the remaining power by discharging. At t = 5s, the PV could have produced 1000W. However, there was no need for the whole PV generation since the load was less than the generation and the SOC was high and around 95%, so the PV generation was curtailed accordingly as per the FLC command. At the same time, there was no power provided by the battery. To assess the performance of the FLC with even lower load than previously considered, the same PV's profile was repeated again for the period from t = 6s to 9s. Again, when there was no power generation from the PV at t = 6s, the whole power was supplied by the battery. Then, the generated PV power became sufficient for the load at t = 7s, so the battery didn't provide any further power. With a higher available power from the PV in comparison to the load, the PV generation was curtailed at t = 8s. At the same time, there was no power provided by the battery and the surplus generated power by the PV was used for charging the battery. When the load was dropped to zero for the period from t = 9 to 12s, the PV generation was further curtailed as per the FLC command and became around 100W only. At the same time, there was no power provided by the battery. As can be seen from Fig. 10(a), the curtailed PV power and original/available PV power are shown in dotted line and solid line respectively. Fig. 10(b) shows the battery and PV power outputs along with the loads' power and SOC curve for SOC = 80%. At t = 0 to 2s, the PV generation was 1140W (maximum generation) that equal to the total load. The battery didn't provide any power. However, when the PV generation dropped to a very low value at t = 2s, load shedding was done for the normal load as per the FLC command. So, the load became 570W (essential and vital) instead of total load (1140W).

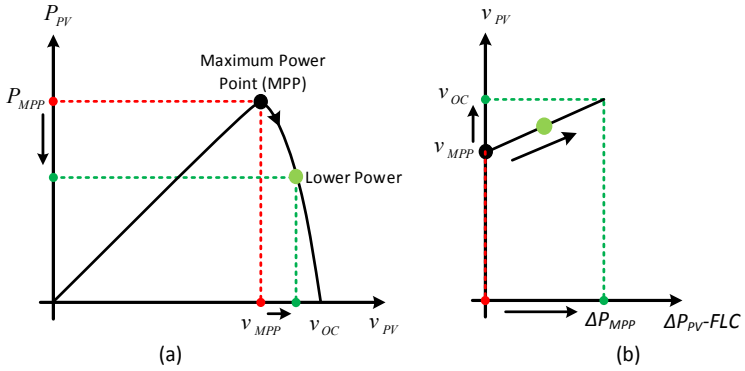

Fig. 6: PV MPP shifting operation: (a) PV power versus output voltage (b) Change of P_{PV} by FLC.

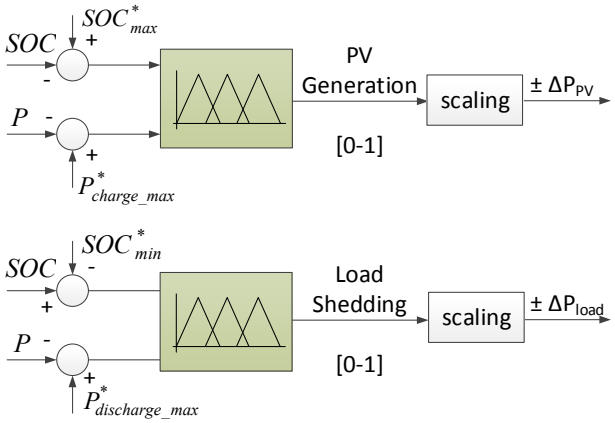

Fig. 7: Proposed fuzzy controller

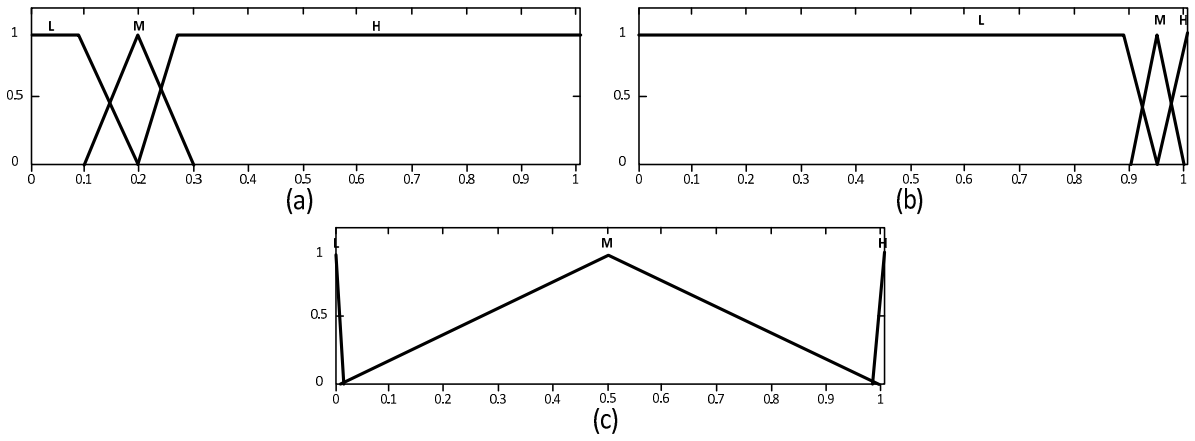

Fig. 8: Membership functions of top FLC: (a) Input-ΔSOC (b) Input-ΔP_{charge} (c) Output-ΔP_{PV}

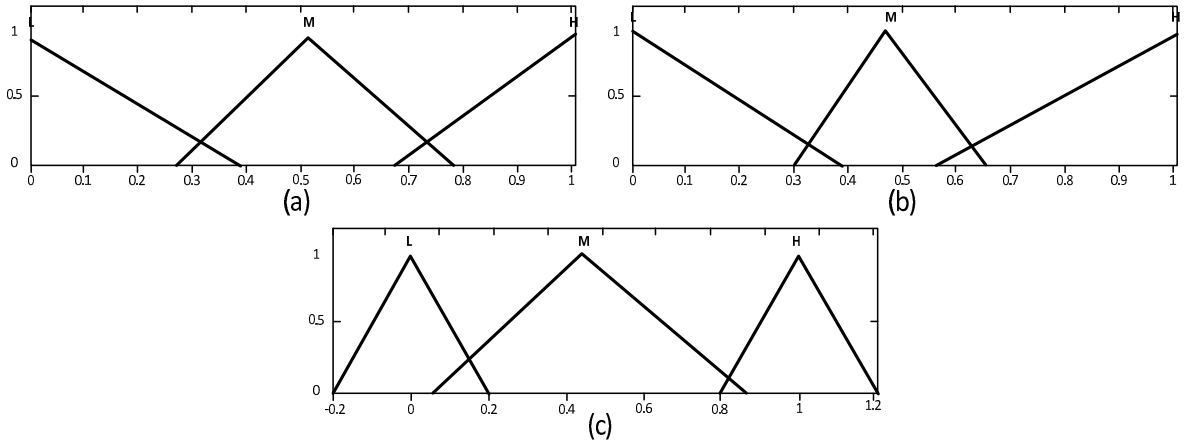

Fig. 9: Membership functions of top FLC: (a) Input-ΔSOC (b) Input-$\Delta P_{discharge}$ (c) Output-ΔP_{Load}

Table II: State of charge and power limits

Parameter	Symbol	Value
Maximum state of charge	SOC^*_{max}	95%
Minimum state of charge	SOC^*_{min}	40%
Maximum charging power	$P^*_{Charge\_max}$	1000W
Maximum discharging power	$P^*_{Discharge\_max}$	1000W

Table III: Rules of top FLC

ΔP_{PV}		ΔP_{charge}		
		L	M	H
ΔSOC	L	L	M	H
	M	M	H	H
	H	M	H	H

Table IV: Rules of bottom FLC

ΔP_{Load}		$\Delta P_{discharge}$		
		L	M	H
ΔSOC	L	L	L	L
	M	M	M	M
	H	H	H	H

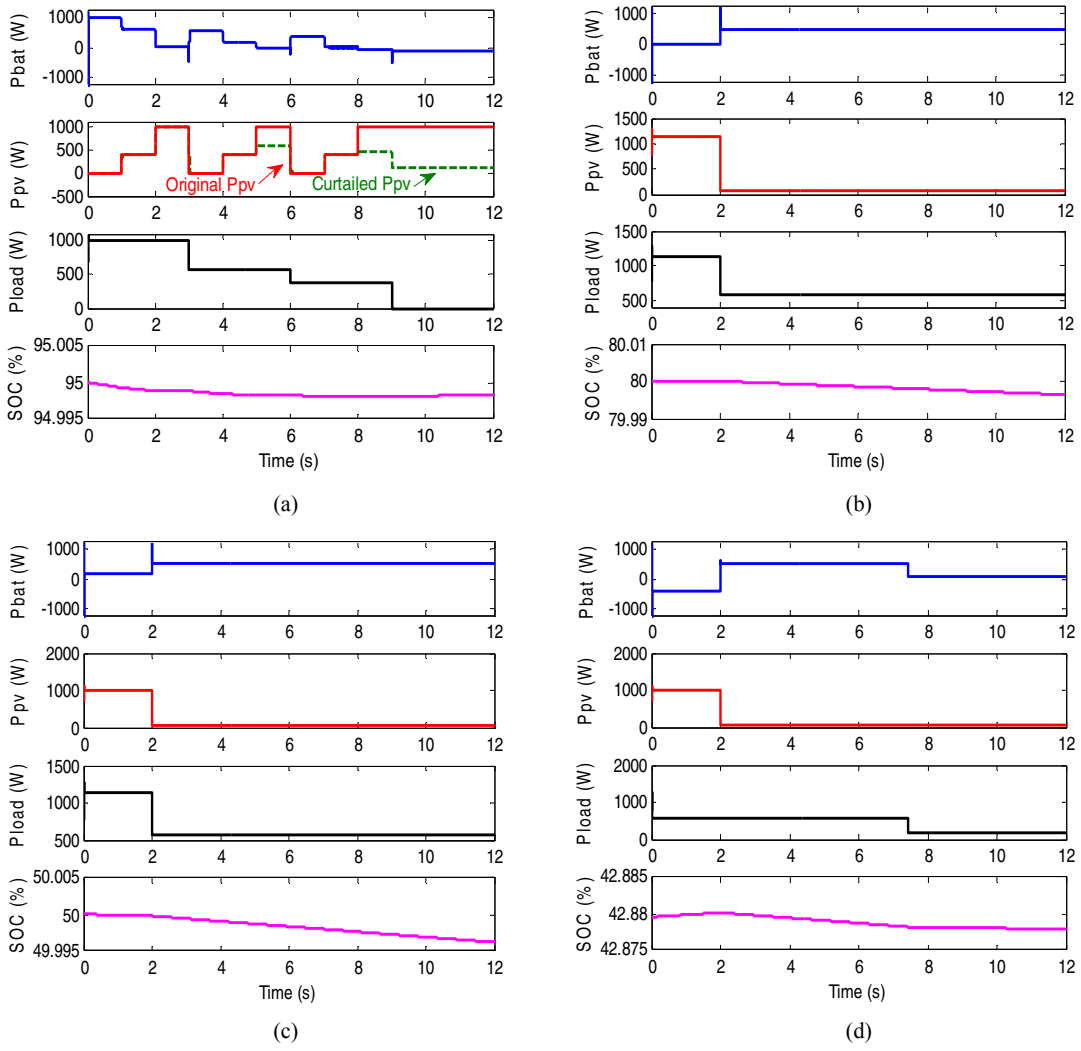

Fig. 10: Battery, PV and load Powers (a) SOC=95% (b) SOC=80% (c) SOC=50% (d) SOC=42.88%

Fig. 10(c) shows the battery and PV power outputs along with the loads' power and SOC curve for SOC = 50%. At t = 0 to 2s, the PV generation was 1000W while the load was 1140W. So, the battery provided 140W. At t = 2s, the PV generation dropped to a very low value. Hence, shedding was done for the normal load as per the FLC command and the load became 570W (essential and vital loads only) instead of total load (1140W). Fig. 10(d) shows the battery and PV power outputs along with the loads' power and SOC curve for SOC = 42.88%. At t = 0 to 2s, the PV generation was 1000W while the load was 570W (essential and vital). There was no power from the battery. At t = 2s, the PV generation dropped to a very low value. The battery managed to provide the required extra power for the load up to around 7.4s since the SOC was still above the minimum allowable limit. However, at

around 7.4s, load shedding was carried out for the essential load as per the FLC command and the load became 170W (vital load only) instead of 570W to keep the SOC of the battery within its design margin. As can be seen from the above results, the SOC and charging / discharging power of the battery were maintained within their design margins for all cases.

Conclusion

A fuzzy logic controller has been proposed for DC microgrid to coordinate the power flow between PV-based RES and Battery-based ESS in island mode. The proposed controller provides an efficient use of the PV's and battery's powers in order to keep the SOC and charging / discharging power of the battery within their required margins regardless of variations in load and intermittent power of renewable energy sources. If necessary, loads' shedding is done whenever required to prevent SOC from exceeding the lower limit and PV curtailment is carried out to realize over charging protection. The power management controller was implemented in a secondary control level to maintain the stability in transients and to provide efficient reference values for steady state operation. Matlab/Simulink results validated the performance of the proposed FLC.

References

[1] Issa W. R., Abusara M. A., and Sharkh S. M.: Control of transient power during unintentional islanding of microgrids, IEEE Trans. Power Electron., Vol. 30 no 8, pp. 4573–4584, 2015

[2] Dragicevic T., Guerrero J. M., Vasquez J. C., and Skrlec D.: Supervisory control of an adaptive-droop regulated DC microgrid with battery management capability, IEEE Trans. Power Electron. Vol. 29 no 2, pp. 695–706, 2014

[3] AlBadwawi R., Abusara M., and Mallick T.: A review of hybrid solar PV and wind energy system, Smart Sci. Vol. 3 no 3, pp. 127–138, 2015

[4] Suganthi L., Iniyan S., and Samuel A. A.: Applications of fuzzy logic in renewable energy systems – A review, Renew. Sustain. Energy Rev. Vol. 48, pp. 585–607, 2015

[5] Cheikh M., Larbes C., Tchoketch G., and Zerguerras A.: Maximum power point tracking using a fuzzy logic control scheme, Rev. des energies, Vol. 10, pp. 387–395, 2007

[6] Bigdeli N.: Optimal management of hybrid PV/fuel cell/battery power system: A comparison of optimal hybrid approaches, Renew. Sustain. Energy Rev., Vol. 42, pp. 377–393, 2015

[7] Esram T. and Chapman P. L.: Comparison of photovoltaic array maximum power point tracking techniques, IEEE Trans. Energy Convers., Vol. 22, no 2, pp. 439–449, 2007

[8] Cheng M.-W., Wang S.-M., Lee Y.-S., and Hsiao S.-H.: Fuzzy controlled fast charging system for lithium-ion batteries, International Conference on Power Electronics and Drive Systems (PEDS), pp. 1498–1503, 2009

[9] Chen Y., Wu Y., and Song C.: Design and implementation of energy management system with fuzzy control for DC micro-grid systems, IEEE Trans. Power Electron., Vol. 28, no 4, pp. 1563–1570, 2012

[10] Diaz N. L., Dragicevic T., Vasquez J. C., and Guerrero J. M.: Fuzzy-logic-based gain-scheduling control for state-of-charge balance of distributed energy storage systems for DC microgrids, Appl. Power Electron. Conf. Expo. (APEC), Twenty-Ninth Annu. IEEE, pp. 2171–2176, 2014

[11] Li X., Hui D., Wu L., and Lai X.: Control strategy of battery state of charge for wind/battery hybrid power system, IEEE Int. Symp. Ind. Electron., no 1, pp. 2723–2726, 2010

[12] Ben Salah C. and Ouali M.: Energy management of a hybrid photovoltaic system, Int. J. Energy Res., Vol. 36, pp. 130–138, 2012

[13] Hassanzadeh A., Monfared M., Golestan S., and Dowlatabadi R.: Small signal averaged model of DC choppers for control studies, Proc. 2011 Int. Conf. Electr. Eng. Informatics, ICEEI, pp. 17–20, 2011

[14] Mahmood H., Michaelson D., and Jiang J.: Control strategy for a standalone PV/battery hybrid system, 38th Annu. Conf. IECON 2012 Proc. (Industrial Electron. Conf.), pp. 3412–3418, 2012

[15] Weidong X., Dunford W. G., Palmer P. R., Capel A., Xiao W.: "Regulation of Photovoltaic Voltage," Ind. Electron. IEEE Trans., vol. 54, no 3, pp. 1365–1374, 2007